Equilibrium and Kinetics of Adsorption of Freon-12 at Infinite Dilution

T. C. Golden and S. Sircar
Air Products and Chemicals, Inc., Allentown, PA 18195

Equilibrium and kinetic data for adsorption of trace CF_2Cl_2 (Freon-12) from various carrier gases on BPL activated carbon are reported. Coadsorption of the bulk carrier gas can severely reduce the equilibrium adsorption capacity and adsorptive mass-transfer coefficient of strongly adsorbed CF_2Cl_2. The difference in size between CF_2Cl_2 and the bulk carrier gas molecules plays a major role in establishing the binary or multicomponent equilibrium adsorption properties. The multisite (single and multicomponent) Langmuir model, which accounts for differences in adsorbate sizes, provides a reasonable framework for describing the size effects. The adsorptive mass transfer of CF_2Cl_2 under the experimental conditions investigated is dominated by surface diffusion into the pores of the activated carbon. The surface diffusivity is a strong function of the extent of coverage and strength of adsorption of the bulk components.

Introduction

Removal of trace impurities from a bulk gas by selective adsorption is a common chemical engineering practice. A pressure swing adsorption (PSA) or a thermal swing adsorption (TSA) process is frequently employed. Design of these processes requires that the equilibrium adsorption capacities and the adsorptive mass-transfer characteristics of the impurities from the bulk gas components be accurately known at the conditions of adsorption and desorption steps of the processes. These conditions can extend over a wide range of pressure, temperature, and impurity concentrations.

There can be significant coadsorption of the bulk gas components even when the selectivities of adsorption of the impurities are moderate to high. This can drastically reduce the adsorption capacities and effective adsorptive mass-transfer coefficients for the trace components. Unfortunately, *a priori* calculation of the effects of coadsorption of the bulk components may not always be possible, particularly when the bulk gas and impurity molecules are very dissimilar in size and polarity, and when the adsorbent is energetically heterogeneous.

The purpose of this article is to study the effects of coadsorption of smaller bulk gas molecules like helium, nitrogen, methane, and carbon dioxide on equilibrium and kinetics of adsorption of larger and more strongly adsorbed Freon-12 (CF_2Cl_2) molecules at trace compositions on a microporous activated carbon.

Correspondence concerning this article should be addressed to S. Sircar.

Experimental

The equilibrium capacities and overall mass-transfer coefficients for adsorption of trace Freon-12 from pure bulk helium, nitrogen, and carbon dioxide as well as from methane (57.0 mol %) + carbon dioxide binary mixture were measured at 310.9 K on BPL carbon (Calgon Corporation) at different total gas pressures using a closed-loop recycle apparatus. The carbon particles were granular (6 × 16 mesh) having a mean particle radius of 0.1 cm. About 60% of the pore volume of the carbon was contained in pores below 40 Å in diameter (Calgon, 1983).

Table 1 shows the physical properties of the adsorbates used in this work (Breck, 1974; Weast, 1977; Moelwyn-Hughes, 1961). Freon-12 is the largest and most polar molecule having a very large dipole moment. It also has the largest polarizability among the adsorbates listed in Table 1. The bulk gas molecules have similar sizes and polarizabilities, but they are approximately 2–2.5 times smaller in size than Freon-12, as indicated by the ratios of their liquid molar volumes at their normal boiling points. The bulk gas molecules range between nonpolar (He, CH_4) to weakly polar (N_2, CO_2) relative to Freon-12. Therefore, Freon-12 is expected to adsorb very selectively from

Table 1. Physical Properties of Adsorbates

Gas	Liquid Molar Vol.* (cm^3/mol)	Dipole Moment (Debye)	Quadrupole Moment ($Å)^3$	Polarizability ($\times 10^{25}$ cm^3)	Molec. Dia. (nm)
CF_2Cl_2	80.7	0.51		71.3	0.44
CO_2	40.0	0	0.64	26.5	0.33
CH_4	37.7	0	0.00	26.0	0.38
N_2	34.7	0	0.31	17.6	0.36
He	32.8	0	0.00	2.0	0.26

* At normal boiling point.

the bulk gases of Table 1. The systems studied in this work, however, provide a significant difference between the sizes and polarities of the selectively adsorbed component and those of the bulk gas components.

Figure 1 is a schematic flow diagram of the apparatus. It consisted of an adsorbent chamber, a stainless-steel bellows recirculating pump (Metal Bellows), a flowmeter, a gas preheater, two small gas holders, a pressure gauge, a set of thermocouples, two sample ports, and several two- and three-way control valves in a closed-loop arrangement. It also contained a bypass line which allowed the gas to be circulated without flowing it through the adsorbent chamber. The entire apparatus was enclosed in a thermostated air bath to maintain a constant temperature (T) during the experiments. A small quantity of adsorbent (~ 5 g) was packed in the adsorption chamber, and a relatively high gas circulation rate was used during the ad(de)sorption experiments so that the difference in the gas composition across the carbon bed was negligible. The sectional void volumes of the adsorbent chamber containing the carbon, the bypass line, and the rest of the apparatus were measured by filling the entire apparatus with helium to a superambient pressure level and successively letting the pressure down to ambient pressure level in different sections of the apparatus and monitoring the quantity of helium leaving the system through a dry test meter.

The ad(de)sorption experiment consisted of filling the entire volume of the evacuated apparatus with the bulk gas (pure or mixture) at the total pressure (P) of the isotherm and circulating the gas through the adsorbent chamber for a period of time in order to ensure that the adsorbent was in equilibrium with the bulk gas at P and T. A known quantity of Freon-12 was then injected into the system while circulating the gas through the bypass loop only, and the initial composition of the Freon-12 in the gas phase was measured by withdrawing a microsample with a syringe. A chromatograph with a flame ionization detector was used for gas analysis. The path of gas circulation was then changed by cutting off the bypass line and flowing the gas over the adsorbent. The gas-phase mole fraction (y_1) of Freon-12 (component 1) was then measured as a function of time (t) by periodically withdrawing microsamples of the gas from the system until equilibrium was attained (no change in y_1 with t). The system pressure remained essentially constant during the entire experiment. The adsorption experiments were repeated after attainment of each equilibrium point by introducing a fresh quantity of Freon-12 into the system. Desorption experiments were carried out by: (a) closing off the adsorbent chamber after an equilibrium state was reached; (b) evacuating the bypass line and the rest of the apparatus; (c) filling the latter two sections with Freon-free bulk gas at pressure P; (d) recirculating the gas over the adsorbent chamber with the bypass line closed; and (e) monitoring the gas-phase Freon-12 composition with time until a new equilibrium was reached.

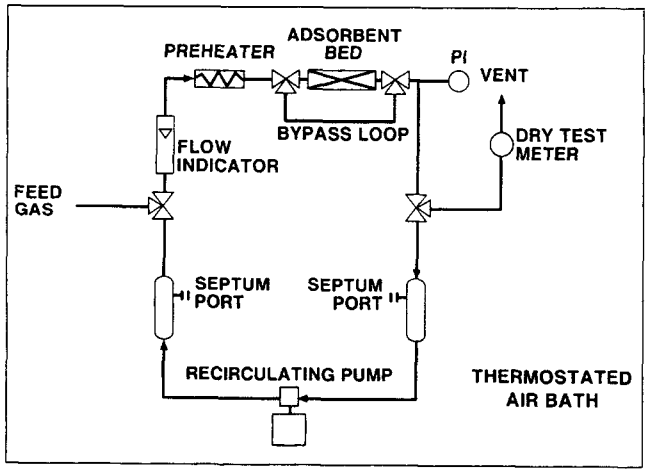

Figure 1. Recirculating apparatus used to measure equilibrium and kinetic data.

Blank experiments were carried out (without the carbon in the adsorbent chamber) to estimate the gas mixing time between the adsorbent chamber and the rest of the apparatus by filling these two sections of the apparatus with gases of different compositions at same P and monitoring the gas composition after the recirculation pump was started. The mixing time was typically found to be less than 5 s as determined by GC samples taken at different time intervals. The specific amount ($\bar{n}_1$) of Freon-12 adsorbed (mol/kg) at time t of the experiment was calculated by:

$$\bar{n}_1(t) = \frac{PV}{WRT}[y_1^0 - y_1(t)] + n_1^{s*}(y_1^s) \tag{1}$$

Where V is the total gas-phase volume (L) in the apparatus excluding the bypass line, W is the amount (kg) of adsorbent in the system, and R is the gas constant. y_1^0 and y_1 are, respectively, the initial mixed gas mole fraction of Freon-12 at the beginning ($t=0$) of the ad(de)sorption experiment and that at time t. n_1^{s*} is the specific equilibrium amount of Freon-12 adsorbed at $t=0$. y_1^s is the gas-phase mole fraction of Freon-12 in the adsorption chamber at $t=0$. Thus, n_1^{s*} is the equilibrium amount of Freon-12 adsorbed at y_1^s, P, and T. y_1^s and n_1^{s*} are equal to zero when the adsorbent is free of Freon-12 at $t=0$. y_1^0 is calculated by measuring the mole fraction of Freon-12 (y_1^b) in the bypass loop at the start of an experiment, and knowing y_1^s and the void volumes of different sections of the apparatus. The experiment is designed to measure the mass-transfer characteristics for ad(de)sorption of trace Freon-12 on the carbon at a constant loading of the bulk gas components at constant values of P and T.

The pure gas adsorption isotherms of nitrogen, methane, and carbon dioxide on BPL carbon were also measured at 303.1 and 343.1 K over a pressure range of 0.1–60.0 atmospheres in a separate set of experiments using a static volumetric adsorption apparatus (Yang, 1987). Furthermore, the binary bulk gas adsorption isotherms of carbon dioxide (1)-methane

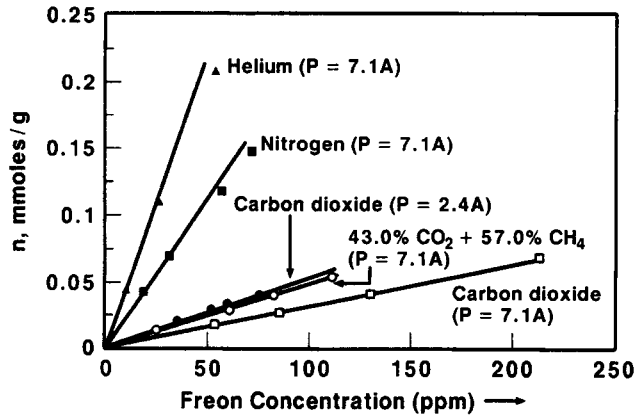

Figure 2. Trace Freon-12 adsorption isotherms from bulk gas mixtures on BPL carbon at 310.9 K.

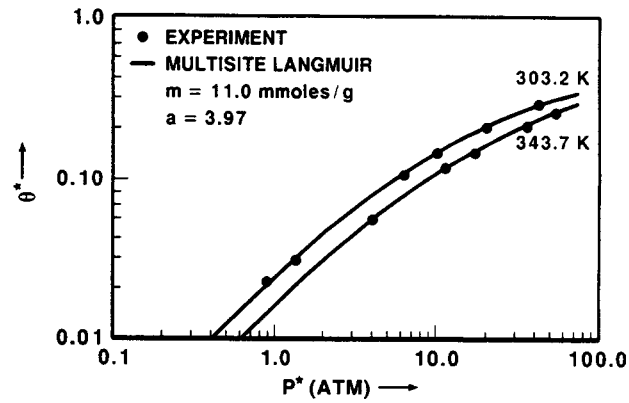

Figure 3. Pure nitrogen adsorption isotherms on BPL carbon at 303.2 and 343.7 K.

(2) mixtures on BPL carbon were measured at 303.1 K and total gas pressure levels of 1.0, 21.3, and 35.0 atmospheres using a desorption technique described elsewhere (Kumar and Sircar, 1986). The binary isotherms were measured at equilibrium CO_2 gas-phase mole fractions of 0.258, 0.478, and 0.748.

The pure gas adsorption isotherm of Freon-12 on BPL carbon was also measured at a temperature of 310.9 K and over a pressure range of 0.0006 to 1.0 atm by a conventional gravimetric method using a microbalance (Yang, 1987).

Equilibrium Adsorption Isotherms

Figure 2 shows the measured isotherms for adsorption of trace (0–200 ppm) Freon-12 from various bulk gases at 310.9 K. The total gas pressure (P) for all experiments was 7.1 atmospheres except for the case of carbon dioxide where total pressures of 2.4 and 7.1 atmospheres were used. The data of Figure 2 include both adsorption and desorption points indicating that the isotherms were reversible.

It may be seen from Figure 2 that the Freon-12 isotherms are linear in the range of the data (Henry's law region). Consequently, they can be represented by:

$$n_1 = K_1 P y_1 \qquad (2)$$

Where n_1 is the specific amount of Freon-12 adsorbed (mol/kg) at a Freon-12 equilibrium gas-phase mole fraction of y_1 from a multicomponent gas phase at P and T. K_1 is the Henry's law constant (mol/kg/atm) for Freon-12 adsorption from a given bulk gas. K_1 is a function of P and T only.

Table 2 (column 1) reports these experimental K_1 values at 310.9 K. Freon-12 is adsorbed very strongly and selectively from nonadsorbing helium with a K_1 of 620 mol/kg/atm. This value of K_1 should also give the Henry's law constant for pure Freon-12 adsorption on the carbon. However, the K_1 for Freon-12 adsorption decreases substantially as the strength of adsorption of the bulk gas component increases. The Freon-12 K_1 values decrease in the order $He > N_2 > CH_4$-CO_2 mixture $> CO_2$ at a given P. The strength of adsorption of the pure bulk gases on the carbon increase in the order $CO_2 > CH_4 > N_2 > He$. This demonstrates the very strong effect of coadsorption of the bulk gases on equilibrium adsorption of trace Freon-12 on the carbon. In particular, the coadsorption of CO_2 at 7.1 atmospheres reduces the Henry's Law constant for Freon-12 adsorption by an order of magnitude compared to that for pure Freon-12 adsorption. The table also shows that the reduction of K_1 for Freon-12 adsorption from CO_2 is a strong function of CO_2 loading. It is reduced by only a factor of three when the CO_2 gas pressure is 2.4 atm.

Table 2. Henry's Law Constants for Freon-12 Adsorption at 310.9 K

	K_1 (mol/kg/atm)			
		IAST		
Bulk Gas	Exp.	Eq. 15	Eqs. 9 and 12	MSL
Helium (7.1A)	620	—	—	—
Nitrogen (7.1A)	310	501	250	298
Carbon Dioxide (2.4A)	220	453	80	151
Carbon Dioxide (7.1A)	46	386	20	40
$CO_2 + CH_4$ (57%) (7.1A)	70	453	37	64

Figures 3, 4, and 5, respectively, show the experimental (circles) pure bulk gas adsorption isotherms of nitrogen, methane, and carbon dioxide on BPL carbon at two temperatures. They are plotted as log θ_i^* against log P_i^* in order to cover three decades of equilibrium gas pressures. θ_i^* is the equilibrium fractional coverage (defined by $\theta_i^* = n_i^*/m_i$). n_i^* is the specific amount of pure gas i adsorbed (mol/kg) at P and T, and m_i is the saturation adsorption capacity (mol/kg) of the pure gas i. The m_i values for the different gases are given in the figures.

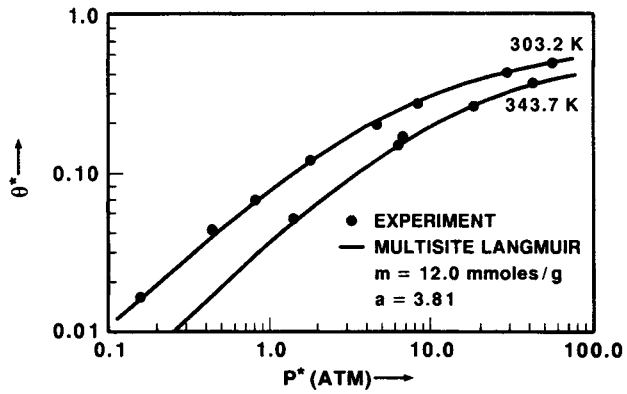

Figure 4. Pure methane adsorption isotherms on BPL carbon 303.2 and 343.7 K.

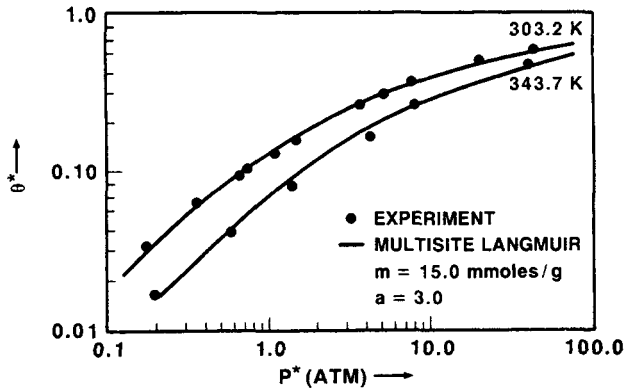

Figure 5. Pure carbon dioxide adsorption isotherms on BPL carbon at 303.2 and 343.7 K.

The isotherms are Type I by Bruauner classification, which is expected for adsorption on microporous adsorbents.

The Henry's law constants $[K_i^* = (\partial n_i^*/\partial P_i^*)_T$ at $P_i^* \to 0]$ for the pure bulk gas adsorption on the carbon were estimated from the isotherms of Figures 3-5. They are reported in Table 3. The isosteric heats of adsorption at zero coverages (q_i^0, kcal/mol) for the pure bulk gases were estimated from the thermodynamic relationship (Sircar, 1985):

$$\frac{d \ln K_i^*}{dT} = -\frac{q_i^0}{RT^2} \tag{3}$$

$$K_i^* = K_i^0 \exp [q_i^0/RT] \tag{4}$$

where K_i^0 is the limiting value of K_i^* at $T \to \infty$. Table 3 reports the values of K_i^0 and q_i^0 for the pure bulk gases. It also gives the value of K_i^* for the gases at 310.9 K estimated by Eq. 4. The K_i^* values for adsorption of pure gases on the carbon increase in the order $CO_2 > CH_4 > N_2$, which also gives their relative strengths of adsorption.

Table 4 reports the experimentally measured binary adsorption isotherms for the bulk $CO_2(1) + CH_4(2)$ mixtures on BPL carbon at 303.1 K and three different total gas pressures. The data are given as fractional coverages ($\theta_i = n_i/m_i$) of component i. n_i is the specific amount adsorbed (mol/kg) for component i and m_i is the corresponding pure component saturation adsorption capacity which is given in Figures 3-5.

Figure 6 shows the experimental (circles) pure Freon-12 adsorption isotherm on BPL carbon at 310.9 K. It is also plotted as log θ_i^* against log P_i^*. The saturation adsorption capacity of Freon-12 is 6.5 mol/kg which is about two times smaller than those for pure CO_2, CH_4, and N_2 adsorption. The Freon-12 isotherm is also Type I in shape. The estimated Henry's law constant is 630 mol/kg/atmosphere, which compares extremely well with that measured from Freon-12/helium binary isotherm, as reported in Table 2.

Table 3. Henry's Law Constants for Adsorption of Pure Gases on BPL Carbon

	(mol/kg/atm)				
	K_i^*			K_i^0	q_i^0 (kcal/mol)
	303 K	343 K	310.9 K		
N_2	0.30	0.18	0.27	4.74×10^{-3}	2.49
CH_4	1.29	0.83	1.05	0.35×10^{-3}	4.94
CO_2	2.88	1.23	2.40	2.11×10^{-3}	4.35
Freon-12	—	—	630.0	—	—

Table 4. Binary $CO_2(1) + CH_4(2)$ Mixture Adsorption Isotherm on BPL Carbon at 30°C

Gas Pres. (atm)	y_1	θ_1 Expt.	θ_1 MSL	Error	θ_2 Expt.	θ_2 MSL	Error
1.0	0.000	0.000	0.000	—	0.080	0.077	−3.9%
	0.258	0.033	0.037	11.4%	0.053	0.055	−3.8%
	0.478	0.066	0.066	0.0%	0.030	0.037	19.3%
	0.748	0.093	0.099	6.4%	0.016	0.017	7.0%
	1.000	0.121	0.129	6.2%	0.000	0.000	—
21.3	0.000	0.000	0.000	—	0.383	0.380	−0.8%
	0.258	0.175	0.206	15.2%	0.192	0.214	10.5%
	0.478	0.309	0.326	5.1%	0.091	0.121	24.6%
	0.748	0.407	0.431	5.6%	0.043	0.048	10.1%
	1.000	0.513	0.500	−2.6%	0.000	0.000	—
35.0	0.000	0.000	0.000	—	0.433	0.435	0.5%
	0.258	0.209	0.245	14.6%	0.220	0.234	5.9%
	0.478	0.369	0.379	2.7%	0.093	0.131	29.3%
	0.748	0.478	0.490	2.5%	0.033	0.049	32.8%
	1.000	0.580	0.560	0.6%	0.000	0.000	—
			Avg.	±6.1%		Avg.	±12.4%

Kinetics of Adsorption of Trace Freon-12

An overall mass-transfer coefficient (k_0, s^{-1}) was evaluated for adsorption of trace Freon-12 from each of the bulk gases on BPL carbon by using a linear driving force (LDF) model. It assumes that the instantaneous rate of adsorption of Freon-12 in the kinetic experiment described earlier is given by:

$$J_1 = \frac{d\bar{n}_1(t)}{dt} = k_0[n_1(y_1) - \bar{n}_1(t)] \tag{5}$$

$\bar{n}_1(t)$ is the specific amount of Freon-12 adsorbed at time t of the experiment which can be calculated by Eq. 1. $n_1 = (K_1 P y_1)$ is the specific equilibrium adsorption capacity of Freon-12 at time t when the transient gas-phase mole fraction of Freon-12 is y_1. J_1 is the instantaneous specific rate (mol/kg/s) of adsorption of Freon-12.

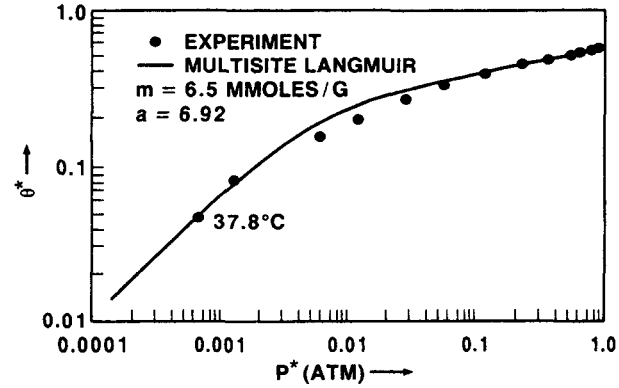

Figure 6. Pure Freon-12 (CF_2Cl_2) adsorption isotherm on BPL carbon at 310.9 K.

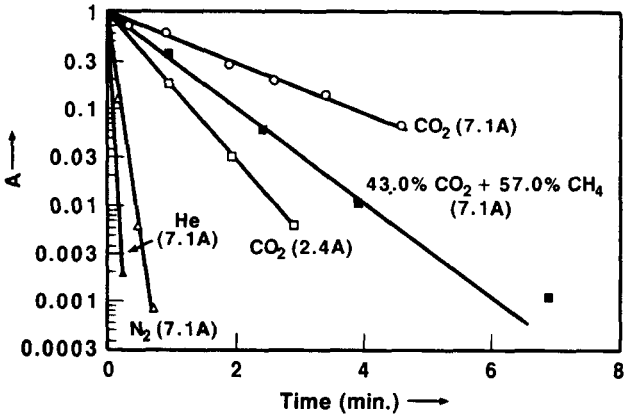

Figure 7. Uptake of trace Freon-12 on BPL from various bulk gases at 310.9 K.

For the kinetic measurements where the adsorbent is free of Freon-12 ($n_i^s = 0$) at the beginning of the test, Eqs. 1, 2, and 5 can be combined and integrated to get:

$$\ln A = -k_0(\beta + 1)t \tag{6}$$

Where A is given by $[(y_1(t)/y_1^0) - \{1/(\beta+1)\}]/[\beta/(\beta+1)]$, and β is equal to $[WK_1RT/V]$. K_1 is the Henry's law constant for Freon-12 adsorption from the appropriate bulk gas. It follows from Eq. 6 that a plot of log A against t would give a straight line with a slope equal to $-k_o[\beta+1]$ and intercept of $A=1$ at $t=0$. Consequently, k_o can be estimated from that plot.

Figure 7 shows a family of plots of log A against t for the Freon-12 adsorption kinetic tests from various bulk gases at 310.9 K and at different total gas pressures. These tests were carried out using a clean adsorbent in the apparatus. The figure shows that the plots are indeed linear over a large range of A values. The striking differences in the slopes of these lines indicate that the mass-transfer rates for adsorption of trace Freon-12 into the carbon are significantly affected by the coadsorption of the bulk gas. Table 5 reports the overall mass-transfer coefficients (k_o) measured in this work. It may be seen that k_o for adsorption of Freon-12 from helium is very large, but it decreases substantially as the strength of adsorption of the bulk gas increases.

Analysis of Equilibrium and Kinetic Data

Equilibrium adsorption of trace Freon-12

The ideal adsorbed solution theory (IAST) of Myers and Prausnitz (1965) was used to explain the decrease in Henry's law constants for adsorption of trace Freon-12 from the bulk gases. For a multicomponent adsorption system, the IAST gives:

$$x_i = \frac{Py_i}{P_i^*} \quad i = 1, 2 \ldots . \tag{7}$$

$$\sum \frac{n_i}{n_i^*(P_i^*)} = 1 \quad i = 1, 2 \ldots . \tag{8}$$

$$\Psi^* = -\frac{\phi}{RT} = -\frac{\phi_i^*}{RT} = \int_o^{P_i^*} \frac{n_i^*}{P_i^*} dP_i^* \quad i = 1, 2 \ldots . \tag{9}$$

Where x_i is the adsorbed phase mole fraction of component i in equilibrium with a gas-phase mole fraction y_i of that component at total gas pressure P and system temperature T. n_i is the specific equilibrium amount of component i adsorbed at P, T, and y_i. n ($=\Sigma n_i$) is the total amount adsorbed ($x_i = n_i/n$). P_i^* is the equilibrium gas-phase pressure of pure component i which gives the same pure gas adsorption surface potential ϕ_i^* as that for the mixture (ϕ) adsorption at P, T, and y_i. $\Psi^*[= -(\phi/RT) = -(\phi_i^*/RT)]$ is the constant of Eq. 9 which can be calculated from either of the pure gas isotherms using the integral of that equation. n_i^* is the specific amount adsorbed of pure component i at P_i^* and T. The model can be used to calculate mixture adsorption isotherms if the pure component adsorption isotherms are known.

For the special case of adsorption of a binary mixture where component 1 is present in trace quantity ($y_1 \to 0$, $y_2 \to 1$), it follows from Eq. 7 that $x_1 \to 0$, $x_2 \to 1$, and $P_2^* \to P$.

Consequently, Eqs. 7 and 8 yield:

$$n_1 = \frac{n_2^*(P) \cdot Py_1}{P_1^*(\Psi^*)} \quad y_1 \to 0 \tag{10}$$

$$n_2 = n_2^*(P) \quad y_1 \to 0 \tag{11}$$

Equation 10 gives the specific amount of component 1 adsorbed from the mixture at the limit of $y_1 \to 0$ at total gas pressure of P. $n_2^*(P)$ is the specific amount of pure component 2 adsorbed at a total gas pressure of P. Equation 11 indicates that the specific amount of component 2 adsorbed from the mixture is equal to that of pure component 2 at P. Comparing Eqs. 2 and 10 one gets:

$$K_1 = n_2^*(P)/P_1^*(\Psi^*) \tag{12}$$

$P_1^*(\Psi^*)$ is the pressure of pure component 1 at which the surface potential (Ψ^*) of the mixture at P and T is equal to those of the pure components at the same T as required by Eq. 9. It also follows from Eq. 9 that:

$$\Psi^* = \int_O^P \frac{n_2^*}{P_2^*} dP_2^* \quad y_1 \to 0,\ P_2^* \to P \tag{13}$$

Thus, Ψ^* can be calculated from the pure component 2 adsorption isotherm for any given total gas pressure P for the mixture.

Table 5. Mass-Transfer Coefficients for Adsorption of Freon-12 on BPL Carbon at 37.8°C

		Mass-Transfer Coeff. (s^{-1})				
Bulk Gas	P (atm)	k_0 ($\times 10^3$)	k_g	k_p ($\times 10^3$)	k_s ($\times 10^3$)	$\frac{J_s}{J_s+J_p}$
He	7.1	16.10	0.02	0.18	390	100%
N_2	7.1	12.30	0.06	0.23	15.1	98%
$CO_2(43\%) + CH_4$	7.1	5.10	0.30	0.08	4.3	84%
CO_2	7.1	3.26	0.51	1.73	1.6	47%
CO_2	2.4	5.30	0.22	0.98	4.5	82%

Equations 12 and 13 can, therefore, be used to calculate K_1 for adsorption of the trace component from a binary gas mixture at any given P and T and the two pure component adsorption isotherms using IAST.

Furthermore, if $P_1^*(\Psi^*)$ is so small that the pure gas adsorption isotherm of component 1 is linear in that pressure region, n_1^* may be written as:

$$n_1^* = K_1^* P_1^* = \Psi^* \tag{14}$$

Where K_1^* is the Henry's Law constant of pure component 1, Eqs. 12-14 can be combined to get:

$$K_1 = K_1^* \cdot \frac{n_2^*(P)}{\Psi^*(P)} \tag{15}$$

Equation 15 is a very interesting result. It shows that K_1 for adsorption of the trace component from a binary mixture can be calculated for any P and T by knowing only the Henry's law constant for component 1 and the adsorption isotherm of component 2 up to pressure P. This can drastically reduce the extent of pure component 1 adsorption isotherm data required for application of IAST for prediction of K_1. Otherwise Eqs. 9 and 12 need to be solved simultaneously using extensive adsorption isotherm data for both components.

We first applied the simple Eq. 15 to calculate K_1 for adsorption of Freon-12 from various bulk gases. K_1^* for Freon-12 was obtained from the data of Figure 2 for adsorption of Freon-12 from helium. n_2^* and ψ^* were calculated using pure component isotherms of the bulk gases (Figures 3-5) and Eq. 9. The column 2 of Table 2 gives the results of these calculations which show that Eq. 15 significantly overpredicts the K_1 values for Freon-12 adsorption from the mixtures. It also fails to predict the order of magnitude of reduction in the Freon-12 K_1 values due to coadsorption of the bulk gas components. The reason for this is that the pure Freon-12 isotherm at 310.9 K is nonlinear, even at very low pressures as shown by Figure 6, and Eqs. 9 and 12 must be used to obtain the correct predictions of Freon-12 K_1 values by the IAST.

Figure 8 shows the calculated values of Ψ^* $(= -\phi_i^*/RT)$ as functions of ln P_i^* for pure gas adsorption of CF_2Cl_2, CO_2, CH_4, and N_2 on the BPL carbon at 310.9 K. They were obtained using Eq. 9 and the isotherms of Figures 3-6. An alternative form of Eq. 9 given below was used to calculate Ψ^* for Freon-12 because the isotherm is very steep at the limit of $P^* \to 0$:

$$\Psi^* = \int_0^{n_i^*(P_i^*)} \left(\frac{\mathrm{dln}\, P_i^*}{\mathrm{dln}\, n_i^*}\right) dn_i^* \tag{16}$$

The integrand of Eq. 16 has a limiting value of unity at the limit of $P_i^* \to 0$ $(n_i^* \to 0)$. This allows reliable extrapolation of the integrand to the lower limit of integration of Eq. 16.

Column 3 of Table 2 shows the results of these rigorous calculations using IAST. The predicted Freon-12 K_1 values now show the right order of reduction due to coadsorption of the bulk components, but their absolute values are much lower than the experimental K_1 values by factors of 1.3-2.8.

For the ternary $CF_2Cl_2(1) + CO_2(2) + CH_4(3)$ system studied in this work, the IAST dictates that $n_2^*(P)$ in Eqs. 12 and 15 be replaced by $(\hat{n}_2 + \hat{n}_3)$ where $\hat{n}_2$ and $\hat{n}_3$ are specific equilibrium

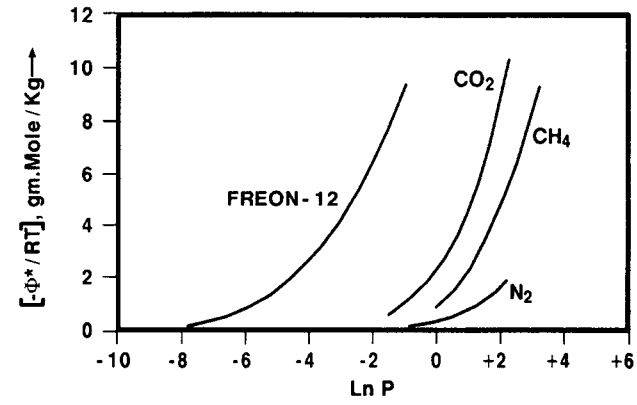

Figure 8. Surface potential of gases on BPL carbon at 310.9 K.

amounts adsorbed of CO_2 and CH_4, respectively, from a bulk binary mixture having CO_2 and CH_4 mole fractions of the Freon-12 free ternary system at P and T of the mixture.

We investigated the cause of underprediction of the Freon-12 K_1 values by the rigorous IAST. A key characteristic of the systems studied was that the more strongly adsorbed species was approximately twice as big as the bulk gas components. Consequently, the multisite Langmuir (MSL) model (Nitta et al., 1984) which describes pure and multicomponent gas adsorption isotherms on energetically homogeneous adsorbents for components having different molecular sizes was chosen for data analysis. The model provides the following set of isotherm equations:

Pure Gas

$$\overline{K}_i^* P_i^* = \theta_i^*/[1-\theta_i^*]^{a_i} \quad i = 1, 2 \ldots \tag{17}$$

$$\theta_i^* = n_i^*/m_i \quad i = 1, 2 \ldots \tag{18}$$

Mixed Gas

$$\overline{K}_i^* P y_1 = \theta_i / \left[1 - \sum_i \theta_i\right]^{a_i} \quad i = 1, 2 \ldots \tag{19}$$

θ_i^* is the fractional amount adsorbed of pure gas i at a gas pressure of P_i^* and temperature T. $\theta_i\,(= n_i/m_i)$ is the fractional amount adsorbed of component i from a gas mixture having a total gas pressure of P and component i gas-phase mole fraction of y_i at temperature T. $\overline{K}_i^*$ is the Henry's law constant for adsorption of pure gas i in the $\theta_i^* - P_i^*$ domain at T $[\overline{K}_i^* = (\partial\theta_i^*/\partial P_i^*)_T$ at $P_i^* \to 0]$. $\overline{K}_i^*$ is related to K_i^* by:

$$K_i^* = \overline{K}_i^* \cdot m_i \tag{20}$$

m_i is the specific saturation adsorption capacity (mol/kg) of pure gas i at T and a_i (sites/mol) is the number of adsorption sites occupied by one mole of that component. m_i and a_i are temperature independent and their product is a constant:

$$a_i \cdot m_i = \text{constant} \tag{21}$$

Equation 21 represents a specific site or adsorption space bal-

ance for the adsorbent. This is a requisite for the MSL model. The temperature dependence of $\overline{K}_i^*$ is given by:

$$\overline{K}_i^* = \overline{K}_i^o \exp\,[q_i^o/RT] \tag{22}$$

$\overline{K}_i^o$ $(=K_i^o/m_i)$ is the limiting value of $\overline{K}_i^*$ at $T\to\infty$. q_i^o is the isosteric heat of adsorption of pure gas i at the limit of zero coverage $(\theta_i^*\to 0)$. It can be shown by using adsorption thermodynamics (Sircar, 1985) that Eqs. 17 and 19 satisfy the isothermal-isobaric thermodynamic consistency test for binary gas adsorption when Eq. 21 is satisfied. Furthermore, thermodynamic calculations (Sircar, 1985) of isosteric heats of adsorption of the pure gases (q_i^*) and those of the components of the gas mixture (q_i) for the MSL model as functions of adsorbate loadings $(\theta_i^*$ or $\theta_i)$ show that:

$$q_i(\theta_i) = q_i^*(\theta_i^*) = q_i^o \tag{23}$$

Thus, the MSL model represents an energetically homogeneous adsorbent. Application of IAST to pure gas adsorption isotherms of MSL (Eq. 17) generate the mixed gas MSL adsorption isotherms (Eq. 19) only when a_i and m_i for all components are equal. Otherwise IAST would predict a θ_i value less than those given by Eq. 19 for any given set of P, T, and y_i.

For adsorption of trace impurity (component 1, $y_1\to 0$) from a multicomponent gas mixture comprising j $(=2, 3\ldots)$ components, Eq. 19 may be rewritten as:

$$\overline{K}_1^* P\cdot y_1 = \theta_1 \Big/ \left[1-\sum_j \theta_j\right]^{a_1} \qquad j=2,\,3\ldots \tag{24}$$

$$\overline{K}_j^* P\cdot y_j = \theta_j \Big/ \left[1-\sum_j \theta_j\right]^{a_j} \qquad j=2,\,3\ldots \tag{25}$$

Equation 24 describes the adsorption isotherm of component 1 at its Henry's Law limit from the multicomponent mixture $(y_1\to 0,\ \theta_1\to 0)$ at total gas pressure of P. Equation 25 gives the coadsorbed amounts of component j. Equations 2 and 24 can be compared to obtain:

$$K_1 = K_1^* \left[1-\sum_j \theta_j\right]^{a_1} \qquad j=2,\,3\ldots \tag{26}$$

According to the MSL model, Eq. 26 can be used to calculate K_1 for Freon-12 adsorption from different bulk gases. For a binary gas mixture $(j=2,\ y_j=1)$, Eqs. 17 and 25 are identical so that the specific amount adsorbed of the bulk gas component becomes equal to that of the pure bulk gas at total system gas pressure as given by Eq. 11.

The pure gas adsorption isotherms of N_2, CH_4, CO_2, and CF_2Cl_2 described by Figures 3–6 were fitted using the pure gas MSL model (Eq. 17). The solid lines in these figures describe the fit. The model can describe these isotherms very well (within experimental error of $\pm 5\%$) over a large range of adsorbate pressures and temperatures. The model parameters $(m_i,\ a_i)$ and $(K_i^o,\ q_i^o)$ are given in the figures and Table 3, respectively. The product $(a_i\cdot m_i)$ was approximately equal to 45.0 sites/g for all adsorbates. The Henry's law constant for pure Freon-12 isotherm at 310.9 K was estimated to be 630 mol/kg/atm which was very close to that obtained from the Freon-12/helium mixed gas isotherm of Figure 2 (Table 2). These results show that BPL carbon acts as a homogeneous adsorbent for the adsorbates evaluated in this work despite the large variation in their molecular sizes and polarities.

The pure component adsorption isotherms for CO_2 and CH_4 were used to calculate binary CO_2-CH_4 adsorption isotherms at different total gas pressures and 303.1 K using Eq. 19. Table 4 compares these calculations with the experimental isotherms. The MSL model predicted the amounts of CO_2 adsorbed from CH_4 fairly well with an average error of $\pm 6.1\%$. CO_2 is the more strongly adsorbed species. The prediction of CH_4 adsorption from CO_2 was not as good having an average error of $\pm 12.4\%$. These errors are, however, as good or better than the predictions of multicomponent adsorption isotherms by other well known models (Valenzuela and Myers, 1984).

The Henry's law constant (K_1) for adsorption of trace Freon-12 from various bulk gases investigated in this work were calculated by the MSL model using the pure gas adsorption isotherms and Eqs. 25 and 26. The column 4 of Table 2 shows the results. It may be seen that the MSL model predicts the experimental K_1 values very well. It somewhat underpredicts the K_1 values (4–15%) for adsorption from N_2, CO_2, and CO_2-CH_4 mixture at 7.1 atm total pressure. The K_1 value for adsorption from CO_2 at 2.4 atmosphere pressure is underpredicted by 45%. This is a marked improvement over the IAST predictions. These results clearly demonstrate the role of the differences in adsorbate sizes on multicomponent adsorption equilibrium which is not always recognized. Similar results have been found for adsorption of other large trace-gas molecules and small carrier-gas molecules (Joseph, 1993). The single-gas and multicomponent-gas MSL model may form a thermodynamically consistent but simple analytical framework to account for the difference in adsorbate sizes. Therefore, the use of the MSL model as a local adsorption isotherm in a patchwise homogeneous framework (Sircar, 1991) of adsorbent heterogeneity may yield an adequately flexible adsorption equation for single- and multicomponent-gas mixtures for practical use.

Kinetics of adsorption of trace Freon-12

The overall mass-transfer coefficients (k_o) for adsorption of trace Freon-12 from various bulk gases estimated by applying Eqs. 5 and 6 to the experimentally measured kinetic data (reported in Table 5) were further analyzed. It was assumed that the overall mass-transfer resistance consisted of an external gas film (outside carbon particle) resistance in series with internal pore diffusion and surface diffusion resistances within the porous carbon particles. The last two resistances operated in parallel. Thus, for an adsorption system where the equilibrium adsorption of Freon-12 was given by a linear isotherm (Eq. 2) and the overall mass transfer was described by the linear driving force model (Eq. 5), the transient rate of Freon-12 adsorption could be written as:

$$J_1 = (ak_f)P[y_1 - y_1^s] = k_o K_1 P[y_1 - \bar{y}_1] \tag{27}$$

$$J_1 = J_{1P} + J_{1S} \tag{28}$$

$$J_{1P} = \bar{k}_P \cdot \frac{P}{RT} \frac{\epsilon - \epsilon_b}{\rho_b} [y_1^s - \bar{y}_1] \tag{29}$$

$$J_{1S} = k_s K_1 P [y_1^s - \bar{y}_1] \tag{30}$$

Where J_1 (mol/kg/s) is the overall transient rate of adsorption of Freon-12. J_{1P} and J_{1S} are, respectively, the internal pore and surface diffusion contributions to the overall rate of adsorption. (ak_f), $\bar{k}_P$ $[=15(D_P/R_P^2)]$ and k_s are, respectively, the external film, internal pore, and surface diffusion mass-transfer coefficients for Freon-12 adsorption. y_1, y_1^s, and $\bar{y}_1$ are, respectively, transient mole fractions of Freon-12 in the bulk gas, at the external surface of the carbon particle and at equilibrium with the transient Freon-12 loading $\bar{n}_1$ $(=K_1 P \bar{y}_1)$ at time t. a $(=3/R_P \rho_P)$ is the external surface area (cm^2/kg) of carbon particles per unit weight of the carbon, and R_P is the radius of the carbon particle. ρ_b and ρ_P are, respectively, the bulk density and the particle density of the carbon. D_P is the diffusivity of Freon-12 into the pores of the carbon at P, T, and $\bar{y}_1$. k_f is the external film mass-transfer coefficient (mol/s/cm^2) per unit external surface area of the carbon particles. ϵ and ϵ_b are, respectively, the total helium and external void fractions within the packed carbon mass used in the kinetic test.

Equations 27-29 can be combined to get:

$$\frac{1}{k_o} = \frac{1}{k_g} + \frac{1}{k_s + k_P} \tag{31}$$

k_g $(=k_f a/K_1)$ and $k_P = [[\bar{k}_p \cdot (\epsilon - \epsilon_b)]/(RT\rho_b K_1)]$ are effective external film and internal pore diffusion mass-transfer coefficients (s^{-1}) for adsorption of Freon-12 in the carbon. k_g can be calculated by conventional correlations (Satterfield, 1970):

$$k_g = \frac{1.071}{K_1 \epsilon_b P R_P \rho_P} G \cdot (Re)^{-0.359} (Sc)^{-0.667} \tag{32}$$

where G is the mass-flow rate (mol/s/cm^2) of gas passing over the carbon particles based on empty cross-sectional area of the adsorbent chamber in the test apparatus. Re and Sc are the gas-phase Reynolds and Schmidts numbers at the flow conditions.

D_P, and consequently k_P, can be calculated by measuring the pore-size distribution of the carbon and using the random pore diffusion model (Wakao and Smith, 1962). BPL carbon has a bimodal pore size distribution as measured by mercury porosimetry (Sircar and Kumar, 1986). The mean pore diameters of the small and the large pore regions are, respectively, 30 Å and 1.4 μm and the corresponding pore void fractions are 0.396 and 0.189. These structural data are sufficient to calculate D_P for any gas diffusing into the pores of the BPL carbon.

k_s can then be evaluated by using Eq. 31 and the experimentally measured k_o values. The values of k_g, k_P, and k_s for the adsorption of trace Freon-12 from various bulk gases are given in Table 5. It may be seen that the effective external film mass-transfer coefficient (k_g) is very large compared to k_o for all cases except for adsorption of Freon-12 from helium where that resistance controls the Freon-12 adsorption. Otherwise, the Freon-12 adsorption is governed by internal resistances.

The last column of Table 5 gives the fraction of total flow of Freon-12 into the pores of BPL carbon caused by surface diffusion from different bulk gases. Surface diffusion controls practically all of internal flux of trace Freon-12 when the bulk gas is very weakly adsorbed (helium and nitrogen). The surface diffusion contribution of internal flux for Freon-12 decreases rapidly when the coadsorption and strength of adsorption of the bulk gas component increases. For example, the surface diffusion contributes to only 82 and 47% of total internal flux when trace Freon-12 is adsorbed from bulk CO_2 at 2.4 and 7.1 atmospheres, respectively. The fractional coverages (θ_2) of CO_2 at these conditions are, respectively, 0.19 and 0.33.

The k_s values reported in Table 5 demonstrate another very interesting feature. The absolute value of k_s for adsorption of trace Freon-12 from helium is relatively very high. It decreases by a factor of 25 when N_2 is the bulk gas at 7.1 atmosphere total gas pressure. The fractional coverage (θ_2) of N_2 at that pressure is only 0.10. On the other hand, k_s for trace Freon-12 decreases by a factor of 85 when CO_2 is the bulk gas at a pressure of 2.4 atmospheres $(\theta_2 = 0.19)$. The most drastic reduction in the k_s value (factor of 240) is observed when CO_2 at 7.1 atm $(\theta_2 = 0.33)$ is the bulk gas. For the case of uptake of trace Freon-12 from a $CO_2(2)$-$CH_4(3)$ mixture at 7.1 atm total pressure $(\theta_2 = 0.18,\ \theta_3 = 0.10)$, the reduction in k_s value was comparable to that from pure CO_2 at a θ_2 of 0.19.

These results indicate that the surface diffusion of trace Freon-12 constitutes the major mode of transport into the pores of BPL carbon. The surface diffusivity or the mass-transfer coefficient for surface flow (k_s) depends very strongly on the nature and extent of the coadsorbed molecules. k_s can decrease by orders of magnitude when the coadsorbed component is relatively strongly adsorbed even at moderate surface coverages by that component.

This phenomenon can be qualitatively explained by a hopping mechanism for surface diffusion. The surface migration of trace Freon-12 is slowed down when a coadsorbed species is present because Freon-12 has to hop to empty sites or displace the coadsorbed component in order to travel on the carbon surface. The larger the population of the coadsorbed molecule and the stronger its adsorption energy, the slower will be the movement of Freon-12 on the surface.

There is very little published literature on surface diffusion of multicomponent mixtures (Karger and Ruthven, 1992). Most of the published literature on surface diffusion deals with single adsorbate systems and the corresponding effect of adsorbate coverage on the surface diffusivity. A vacancy diffusion model of surface diffusion for a binary adsorbate system proposed by Qureshi and Wei (1990) predicts that the effective surface diffusivity of a trace component in presence of a constant adsorbate loading of a second component (present case) should decrease linearly with the fractional coverage of the second component.

Another kinetic model of binary surface diffusion proposed by Chen and Yang (1992), which is based on the classical transition state theory, dictates that the surface diffusivity of a trace component should remain constant or increase with increased coverage of the second component. According to our data, the k_s for Freon-12 decreased approximately exponentially with increased coverage of CO_2 on the carbon.

Our test results show that binary or multicomponent surface diffusion is a very complex phenomenon and the present state of the art does not allow *a priori* prediction of mixed gas surface

diffusivities. More fundamental work including accurate measurements of this property are clearly needed.

Summary

The following key conclusions can be made from the results of this study:

(1) Coadsorption of bulk components can severely reduce the equilibrium adsorption capacity and adsorptive mass-transfer coefficients of strongly adsorbed trace components.

(2) The differences in the sizes of the trace components and the bulk components play a major role in establishing the binary or multicomponent equilibrium adsorption properties. The multisite (single and multicomponent) Langmuir adsorption model, which accounts for differences in adsorbate sizes, provides a reasonable framework for describing the size effects.

(3) Surface diffusion into the pores of activated carbons play a dominant role in determining the overall mass transfer of the trace adsorbates. The surface diffusivity is a strong function of the extent of coverage and strength of adsorption of the bulk components. Existing models for describing this effect may not be adequate.

(4) Models are needed to describe both equilibrium and kinetics of adsorption of multicomponent adsorbates of dissimilar sizes and polarities on heterogeneous adsorbents. Extensive experimental data are needed to test these models.

Notation

a = external surface area of adsorbent particle per unit mass
a_i = adsorption sites per mole of adsorbate i
A = $[(y_1(t)/y_1^o) - \{1/(\beta+1)\}]/[\beta/(\beta+1)]$
D = diffusivity of trace component
D_P = effective pore diffusivity for trace component
G = mass-flow rate of gas in circulating kinetic apparatus
J = flux of trace adsorbate into the carbon
k_o = overall adsorptive mass-transfer coefficient for trace adsorbate
k_f = external film mass-transfer coefficient for trace adsorbate per unit area of adsorbent
k_g = effective external mass-transfer coefficient for trace adsorbate = $(k_f a)/K_1$
$\bar{k}_P$ = internal mass-transfer coefficient for gas-phase diffusion of trace adsorbate in the carbon pores = $15\ D_P/(R_P)^2$
k_P = $\bar{k}_P(\epsilon - \epsilon_b)/K_1\rho_b RT$
k_s = mass-transfer coefficient for surface diffusion of trace adsorbate in the carbon pores
$\underline{K}$ = Henry's law constant
$\bar{K}$ = K/m
K^o = limiting value of K at $T \to \infty$
m = saturation adsorption capacity of the adsorbate
n = specific equilibrium amount adsorbed
n_1^s = specific equilibrium amount of trace component adsorbed at P, T, and y_1^s
$\bar{n}$ = specific transient amount adsorbed
P = total gas pressure
q = isosteric heat of adsorption
q^o = isosteric heat of adsorption at zero coverage
R = gas constant
R_P = adsorbent particle radius
Re = particle Reynolds number = $(2R_P G)/\mu$
Sc = Schmidt number = $\mu/\rho D$
t = time
T = temperature
V = void volume of recirculating test apparatus
x = adsorbed phase mole fraction
y = gas-phase mole fraction
y_1^s = gas-phase mole fraction of trace component in adsorbent chamber of kinetic test at $t = 0$

Greek letters

β = $(WK_1RT)/V$
ϵ = total helium void fraction of carbon bed
ϵ_b = external void fraction of carbon bed
θ = fractional coverage = (n/m)
μ = gas viscosity
ρ = gas density
ρ_b = carbon bulk density
ρ_P = carbon particle density
ϕ = surface potential
ψ^* = $-\phi/RT = -\phi_i^*/RT$

Subscripts

1 = trace adsorbate (component 1)
i = component i
s = surface phase
P = pore phase

Superscripts

* = pure gas properties

Literature Cited

Breck, D. W., *Zeolite Molecular Sieves*, Wiley, New York (1974).

Chen, Y. D., and R. T. Yang, "Predicting Binary Fickian Diffusivities from Pure Component Fickian Diffusivities for Surface Diffusion," *Chem. Eng. Sci.*, **47**, 3895 (1992).

Joseph, J. C., A. L. Myers, T. C. Golden, and S. Sircar, "Adsorption of Trace Gases (Propane, Butane and Freon-12) from Carrier Gases (Helium, Nitrogen and Carbon Dioxide) on Activated Carbon," *J. Chem. Soc. Faraday Trans.*, **89**, 3491 (1993).

Karger, J., and D. M. Ruthven, *Diffusion in Zeolites and Other Microporous Solids*, Wiley, New York (1992).

Kumar, R., and S. Sircar, "Skin Resistance for Adsorbate Mass Transfer Into Extruded Adsorbent Pellets," *Chem. Eng. Sci.*, **41**, 2215 (1986).

Moelwyn-Hughes, E. A., *Physical Chemistry*, 2nd ed., Pergamon Press, New York (1961).

Myers, A. L., and J. M. Prausnitz, "Thermodynamics of Mixed Gas Adsorption," *AIChE J.*, **11**, 121 (1965).

Nitta, T., T. Shigetomi, M. Kuro-oka, and T. Katayama, "An Adsorption Isotherm of Multi-Site Occupancy Model for Homogeneous Surface," *J. Chem. Eng. Japan*, **17**, 39 (1984).

Qureshi, W. R., and J. Wei, "One and Two Component Diffusion in Zeolite ZSM-5, I. Theory," *J. Catal.*, **126**, 126 (1990).

Satterfield, C. N., *Mass Transfer in Heterogeneous Catalysis*, MIT Press, Cambridge, MA (1970).

Sircar, S., "Excess Properties and Thermodynamics of Multicomponent Gas Adsorption," *J. Chem. Soc., Faraday Trans I.*, **81**, 1527 (1985).

Sircar, S., and R. Kumar, "Column Dynamics for Adsorption of Bulk Binary Gas Mixtures on Activated Carbon," *Sep. Sci Tech.*, **21**, 919 (1986).

Sircar, S., "Role of Adsorbent Heterogeneity on Mixed Gas Adsorption," *I&EC Res.*, **30**, 1032 (1991).

"Type BPL Granular Carbon," Calgon Corp. Data Sheet 23-106a (1983).

Valenzuela, D., and A. L. Myers, "Gas Adsorption Equilibrium," *Sep. and Purif. Methods*, **13**, 153 (1984).

Wakao, N., and J. M. Smith, "Diffusion in Catalyst Pellets," *Chem. Eng. Sci.*, **17**, 825 (1962).

Weast, R. C., editor, *CRC Handbook of Chemistry & Physics*, 58th ed., CRC Press, Cleveland (1977).

Yang, R. T., *Gas Separation by Adsorption Process*, Butterworths, Boston (1987).

Manuscript received Mar. 1, 1993, and revision received July 22, 1993.